2020 IEEE International Conference on E-health Networking, Application & Services (HEALTHCOM) | 978-1-7281-6267-6/21/$31.00 ©2021 IEEE | DOI: 10.1109/HEALTHCOM49281.2021.9399020

Optimizing Broad Learning System Hyper-parameters through Particle Swarm Optimization for Predicting COVID-19 in 184 Countries

Choujun Zhan*, Zhengdong Wu†, Quansi Wen‡, Ying Gao‡, Haijun Zhang§
* School of Computing, South China Normal University, Guangzhou, China
†School of Electrical and Computer Engineering, Nanfang College of Sun Yat-Sen University, Guangzhou, China
‡ School of Computer Science and Engineering, South China University of Technology, Guangzhou, China
§ Shenzhen Graduate School, Harbin Institute of Technology, Shenzhen, China
Email: * zchoujun2@gmail.com, † wuzhengdong2@gmail.com, ‡ gaoying@scut.edu.cn

***Abstract*—The Coronavirus Disease 2019 (COVID-19) began to outbreak since December 2019 and widely spread over the world. How to accurately predict the spread of COVID-19 is one of the essential issues for controlling the pandemic. This study establishes a general model that can predict the trend of COVID-19 in a country based on historical COVID-19 data in 184 countries. First, Savitzky-Golay (S-G) filter is utilized to detect multiple waves of COVID-19 in a country. Then, a PSO-SIR (particle swarm optimization susceptible-infected-recovery) model is provided for data augmentation. Finally, a novel PSO-BLS (particle swarm optimization broad learning system) is proposed for predicting the trend of COVID-19. Experimental results show that compared with the deep learning models (ANN, CNN, LSTM, and GRU), the PSO-BLS algorithm has higher accuracy and stability in predicting the number of active infected cases and removed cases.**

***Index Terms*—Covid-19, Broad Learning, Particle Swarm Optimization, Epidemiological model, Forecasting**

I. Introduction

Coronavirus Disease (COVID-19), which is caused by severe acute respiratory syndrome coronavirus 2 (SARS-CoV-2) and has high transmissibility with reproduction number [1], began to outbreak at the end of December 2019 [2]. Evidence indicates that COVID-19 patients, presymptomatic patients, and even asymptomatic patients, who are infected with covid-19 but show no symptoms, all have strong person-to-person transmissibility [3]. The flow of a large amount of COVID-19 patients (including patients in the incubation period, mild patients and asymptomatic patients, etc.) play an essential role in the rapid spread of the virus [4]. When the epidemic outbreak, a larger number of patients experienced severe or critical diseases requiring medical care, which would overwhelm the medical system and finally brings a large number of deaths [5]. Up to Aug 14, 2020, COVID-19 has spread to more than 184 countries and caused 21,036,943 infections, with a death toll of 761,926 [6]. Hence, inferring and predicting the spread of the disease in a country will help set public health policy and contain the spread of COVID-19.

Traditional epidemiological models analyze and predict the spread of an epidemic based on the dynamic changes in the number of infected and removed cases. However, these models assume that the transmission environment is stable and the infection rate of all COVID-19 patients is constant [7]. Public health interventions and control measures, such as mask-wearing, keeping social distance, and handwashing, significantly impact slowing the spread [8]. Strong intervention measures can effectively reduce the spread of the disease, and vice versa will help spread the disease. Traditional epidemiological models are suitable for analyzing and predicting the overall trend of disease transmission when the external environment is stable. In this case, a COVID-19 curve show only a single wave. However, in reality, a COVID-19 curve always has multiple peaks. As the traditional epidemiological models have fixed parameters, these models can describe the first wave well but have difficulty fitting and predicting the second or third wave [9]. Therefore, we must establish a data-driven epidemic model to overcome this problem. Through data augmentation, we can overcome the limitations of traditional epidemic models, improve predictive accuracy, and verify the effectiveness of prevention and control measures.

In this article, based on COVID-19 data in 184 countries, we establish a general model that can predict the number of active infection cases and removed cases. First, we use the Savitzky-Golay (S-G) filter to detect peaks and valleys of outbreaks. The COVID-19 curve can be separated into several segments, containing only a single wave. Then, to improve the generalization ability and robustness

of the model, we combine particle swarm optimization (PSO) [10] and susceptible-infected-recovery (SIR) model [11], [12] to generate a set of "artificial COVID-19 spreading data" for data augmentation. Finally, based on historical data and augmented data, a hybrid broad learning system (BLS) [13], in which PSO is utilized for optimizing the hyper-parameters of BLS, is proposed. Compared with several deep learning models (ANN, CNN, LSTM, and GRU) and BLS, the PSO-BLS model has higher stability, robustness, and accuracy. Additionally, the PSO-BLS model can adapt to complex epidemic disease situations and accurately predict the trend of an epidemic with multiple waves.

II. Framework of Data Augmentation

A. COVID-19 data

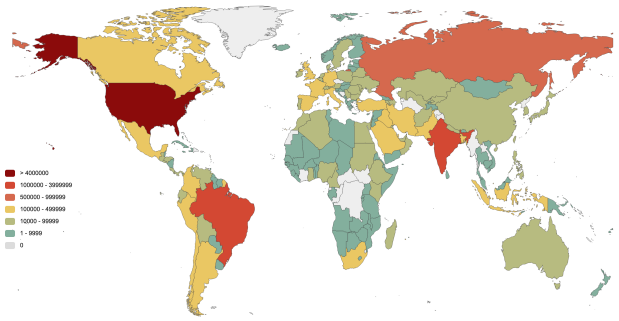

Figure 1. The cumulative number of confirmed cases in 184 countries up to Aug 10, 2020.

Many government facilities (mostly the CDC) release the COVID-19 data to the public [14]. The COVID-19 data utilized in this study include the cumulative number of confirmed, recovered cases, and death tolls for 45 countries in Asia, 46 countries in Europe, 24 countries in North America, 11 countries in South America, 54 countries in Africa, and 4 countries in Oceania. The total population of the 184 countries is 7,730,029,662, accounting for most of the global population. Figure 1 shows the cumulative number of COVID-19 patients in 184 countries.

B. Multiple Waves Detection

A large number of countries, such as Morocco and Croatia, have been hit by a second or even third wave of COVID-19 (shown in Figure II-B). Here, the Savitzky-Golay filter is utilized to detect multiple outbreaks in the historical COVID-19 profiles. Then, based on the detection results, we can divide the historical profile into several segments, in which only a single outbreak happens.

The Savitzky-Golay (S-G) filter, a weighted average convolution algorithm with a moving window based on the time series data smoothing and the polynomial least-squares, can filter out noise, ensuring that the shape and width of the signal remain unchanged [15]. The S-G filter has two parameters, including window size and polynomial order, as shown in the following equation:

$$Y_j^* = \frac{\sum_{i=-m}^{m} C_i \times Y_{j+1}}{2m+1}, \tag{1}$$

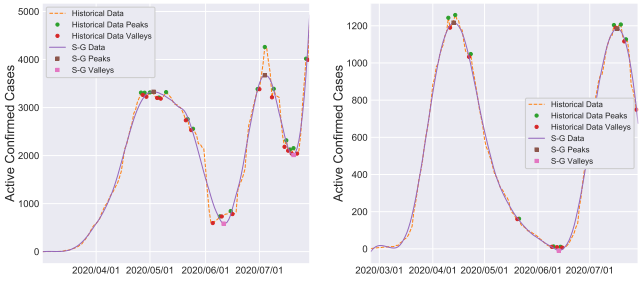

(a) Morocco (b) Croatia

Figure 2. Two illustrative examples of COVID-19 profiles with multiple waves. The dashed line is the historical data, while the solid line represents the filtered line smoothed by S-G filter. The green and red dots stand for the peaks and valleys of historical COVID-19 data, while the brown and pink squares reveal the peaks and valleys of filtered curves, respectively: (a) Morocco; (b) Croatia.

where the Y_j^* is the fitted values, the Y_{j+i} is the signal data, C_i is the coefficient of the $i-th$ value filter, m is the width of half the filter window. Figure II-B shows the historical and filtered curves of active confirmed cases in Morocco and Croatia, respectively. S-G filter successfully smooths the noise and detects the peaks and valleys of each wave. We can then define a segment between two valleys as a wave and separate the whole process into several segments.

C. COVID-19 Data Augmentation

In the traditional SIR model, each individual would be one of the three possible states: susceptible (S), infected (I), and recovered/removed (R) [12], [16]. The onefold SIR model describes the evolution of an epidemic outbreak in terms of a three-order dynamical system. Consider a country or city at time t, the number of susceptible individuals is $S(t)$, the number of infected individuals is $I(t)$, and the number of recovered or removed individuals are $R(t)$. Then, the SIR model takes the following form:

$$\begin{aligned} \frac{dS}{dt} &= \frac{-\beta IS}{N}, \\ \frac{dI}{dt} &= \frac{\beta IS}{N} - \gamma I, \\ \frac{dR}{dt} &= \gamma I, \end{aligned} \tag{2}$$

where β is the rate at which a susceptible individual is infected by a COVID-19 patient, γ is the recovery rate.

Traditional epidemiological models always assume the system is fixed, which means a country or region continuously implements the same epidemic prevention and control measures until totally suppressing the spread of an epidemic. Hence, the parameters of an SIR model, including the infected rate β and recovery rate γ, are fixed. However, in real cases, a country or region will dynamically update intervention measures, resulting in time-varying infected rate $\beta(t)$ and recovery rate $\gamma(t)$. With different public intervention in a region, the trend of COVID-19

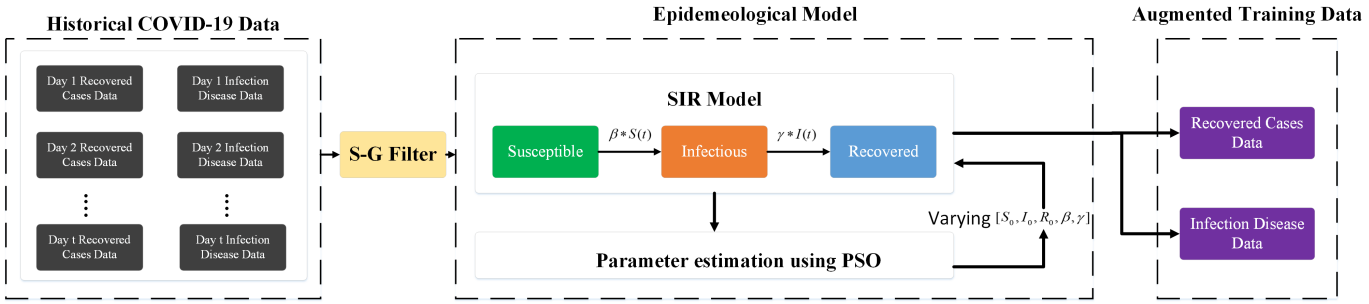

Figure 3. COVID-19 data augmentation through SIR-PSO system.

Algorithm 1 Algorithm for data augmentation through PSO-SIR model.

Input:

The number of infected cases in $N = 184$ countries $I_n(t) = \{I_n(t_0), I_n(t_1), \cdots, I_n(t_T)\}$, where $n = 1, 2, \cdots, 184$.

Output:

Augmented data: $[\hat{I}_1(t), \hat{I}_2(t), \cdots, \hat{I}_{N\times L}(t)]$ and $[\hat{R}_1(t), \hat{R}_2(t), \cdots, \hat{R}_{N\times L}(t)]$

1: Data preprocessing: Divide the original dataset and keep the infection dataset of the first outbreak by using S-G filter.

2: Parameter Identification Process:

for $(n = 0$ to $N - 1)$ **do**

Solve the NLP-(5), where the loss function is as follows:

$$Loss = \sum_{i=1}^{N} w_{ij}(I(t_i) - \hat{I}(t_i\,|\theta))^2$$

end for

return the optimal parameter set $\Theta = \{\theta_1^*, \theta_2^*, \cdots, \theta_N^*\}$.

3: Simulation Data Generation Process:

for $(n = 1$ to $N)$ **do**

for$(i = 0$ to $L - 1)$**do**

$$\theta_{n,i} = \theta_n^* + 0.04(i - m)\theta_n^*$$

. Generate artificial profiles from SIR model based on parameter set $\theta_{n,i}$.

return $[\hat{I}_1(t), \hat{I}_2(t), \cdots, \hat{I}_{N\times L}(t)]$ and $[\hat{R}_1(t), \hat{R}_2(t), \cdots, \hat{R}_{N\times L}(t)]$.

will be time-varying. Hence, historical COVID-19 data of 184 countries can not cover all the possible situations.

Suppose a new wave has happened in a country or region. The historical data of infected and removed cases during the early stage of the spread form an initial trend. We can assume that the new wave will be slightly different from one or several historical waves that happened previously in one or several countries. Then, this initial profile is "similar" with one or several sets of historical profiles. The basic idea of data augmentation is to generate artificial epidemic data from historical data through the SIR model to cover more possible cases. First, for each historical wave, we optimize the key parameters of the SIR model (2) to make the generated growth profile that matches historical cases. Then, we slightly vary the optimal parameter values and generate "artificial profiles" to simulate the effect of different intervention measures and establish a library of spreading profiles covering various possible situations. Thus, a new outbreak would likely follow a combination of several profiles in the library.

Here, we define $S_0 = S(t_0)$, $I_0 = I(t_0)$ and $R_0 = R(t_0)$, which are the initial number of susceptible, infected and recovered individuals in a country or region, respectively. Additionally, The SIR model (2) has two unknown parameters β and γ. In conclusion, the unknown parameter set is:

$$\theta = \{\beta, \gamma, S_0, I_0, R_0\}. \tag{3}$$

Hence, we have to identify a suitable parameter set θ to make the estimated growth trajectory that matches historical data.

Let $X(t)$ be the extended state vector, i.e., $X(t) = [S(t),\ I(t),\ R(t)]$, then, model (2) can be reformulated as:

$$\dot{X}(t) = f(X(t)\,|\theta), \tag{4}$$

where $f(x)$ is the right side of (2). Then, the parameter estimation problem can be formulated as the following constrained nonlinear optimization problem:

$$\begin{aligned} \mathrm{P}_0\colon & \min_{\theta} \sum_{i=1}^{N} w_{ij}(I(t_i) - \hat{I}(t_i\,|\theta))^2 \\ s.t. & \begin{cases} (i) & \dot{X}(t) = f(X(t)\,|\theta). \\ (ii) & \Theta_U \geq \Theta \geq \Theta_L, \end{cases} \end{aligned} \tag{5}$$

where $\hat{I}(t_i\,|\theta)$ represents the estimated number of infected individuals at time t_i with parameter set θ. w_{ij} stands for the weighted coefficient. The searching space of unknown parameter set is bounded between Θ_L and Θ_U. Evolutionary algorithms have been extensively used in nonlinear optimization [17], [18]. Particle Swarm Optimization (PSO) is a global optimization algorithm in order to avoid being trapped in local minima and search the global optima parameters. In this article, PSO is utilized to solve NLP-(5) and find the optimal parameter set θ^* [10]. Then, we expand the a library of different spreading profiles by generate N parameter for each θ^*:

$$\theta_i = \theta^* + 0.04(i - m)\theta^*, \tag{6}$$

where $i = 1, 2, \cdots, 2m$ and $m \geq 1$. In this work, empirically, the ratio in $[0.03, 0.08]$ produces a relatively good result, and the results are robust. Hence, we adopt 0.04 in Eq. (6). Then, we utilize parameter set θ_i and model (2) to generate $2m + 1$ artificial profiles to augment dataset. The specific process is shown in Figure 3.

III. Framework of Hybrid PSO-BLS Model

Algorithm 2 Algorithm for forecasting COVID-19 through the PSO-BLS model.

Input:

Augmented dataset and historical data $[I_1(t), I_2(t), \cdots, I_N(t)]$ and $[R_1(t), R_2(t), \cdots, R_N(t)]$.

Output:

Prediction results: $[\bar{I}_1(t), \bar{I}_2(t) \cdots \bar{I}_N(t)]$ and $[\bar{R}_1(t), \bar{R}_2(t) \cdots \bar{R}_N(t)]$

1: Base on Eq. (7a) and Eq. (7b), restructure the augmented data and historical data to form the training set and testing set:

$$TrainingSet = [\hat{I}(t)_X, \hat{R}(t)_X, \hat{I}(t)_y, \hat{R}(t)_y]$$
$$TestingSet = [I(t)_X, R(t)_X, I(t)_y, R(t)_y]$$

2: Parameter Identification Process:
Input the training set $[\hat{I}(t)_X, \hat{R}(t)_X, \hat{I}(t)_y, \hat{R}(t)_y]$ and testing set $[I(t)_X, R(t)_X, I(t)_y, R(t)_y]$
for $(n = 0$ to $N - 1)$ **do**
Adopt the following loss function and optimize F, W, E, C through PSO:

$$Loss1 = \frac{1}{T}\sum_{i=1}^{T}(I_n(t_i) - \bar{I}_n(t_i))^2,$$
$$Loss2 = \frac{1}{T}\sum_{i=1}^{T}(R_n(t_i) - \bar{R}_n(t_i))^2$$

end for
return optimal initial hyper-parameters $[F_1, F_2, \cdots, F_N]$, $[W_1, W_2, \cdots, W_N]$, $[E_1, E_2, \cdots, E_N]$ and $[C_1, C_2, \cdots, C_N]$.

3: PSO-BLS Prediction Process:
Input the training set $[\hat{I}(t)_X, \hat{R}(t)_X, \hat{I}(t)_y, \hat{R}(t)_y]$ and testing set $[I(t)_X, R(t)_X, I(t)_y, R(t)_y]$;
Input the PSO-BLS parameters $[F_1, F_2, \cdots, F_N]$, $[W_1, W_2, \cdots, W_N]$, $[E_1, E_2, \cdots, E_N]$ and $[C_1, C_2, \cdots, C_N]$.
for $(n = 0$ to $N - 1)$ **do**
Calculate $\bar{I}_i(t) = \{\bar{I}_i(t_0), \bar{I}_i(t_1), \cdots, \bar{I}_i(t_T)\}$ and $\bar{R}_i(t) = \{\bar{R}_i(t_0), \bar{R}_i(t_1), \cdots, \bar{R}_i(t_T)\}$ from BLS model.
return $[\bar{I}_1(t), \bar{I}_2(t) \cdots \bar{I}_N(t)]$ and $[\bar{R}_1(t), \bar{R}_2(t) \cdots \bar{R}_N(t)]$.

In this part, the dataset is reconstructed to meet the multi-step prediction. Since the incubation period of COVID-19 is 14 days, we use the number of active infection cases and the number of removed cases in the past 14 days to predict the number of infections and cures on the seventh day in the future. That is, constructing X with the Equation (7a) and y with the Eq. (7b) as the input of the model.

$$X = \begin{bmatrix} x_1(t-14) & x_1(t-13) & \cdots & x_1(t) \\ x_2(t-14) & x_2(t-13) & \cdots & x_2(t) \\ \vdots & \vdots & \vdots & \vdots \\ x_N(t-14) & x_N(t-13) & \cdots & x_N(t) \end{bmatrix} \tag{7a}$$

$$Y = \left[x_1(t+7), x_2(t+7), \cdots, x_N(t+7)\right] \tag{7b}$$

The Broad Learning System (BLS), a single-layer incremental neural network, is proposed in 2017 [13]. The network is based on a random vector function linked neural network (RVFLNN) [19] and a single layer feedforward neural network (SLFN) [20]. Compared with the deep network model, the BLS are faster convergence, more conciseness, and support for precise accuracy. The input matrix A of BLS is composed of the mapped feature and the enhanced feature. The mapped feature Z is obtained by linear mapping and activation function transformation of the primal matrix.

$$Z_i = \phi(XW_{e_i} + \beta_{e_i}), \qquad i = 1, \cdots, n, \tag{8}$$

where the W and β matrices are randomly generated. We can record the mapping nodes obtained by n times of mapping changes as $Z^n = [Z_1, Z_2, \cdots, Z_n]$. Similarly, the enhanced nodes are transformed by the mapping nodes through linear mapping and activation functions:

$$H_m \equiv \zeta(Z^n W_{h_m} + \beta_{h_m}). \tag{9}$$

Therefore, the model of width learning can be expressed as Eq.(10)

$$\begin{aligned} Y =& [Z_1, Z_2, \cdots, Z_n] | \zeta(Z^n W_{h_1} + \beta_{h_1}), \\ & \cdots, \zeta(Z^n W_{h_m} + \beta_{h_m}) W^m \\ =& [Z_1, Z_2, \cdots, Z_n | H_1, \cdots, H_m] W^m \\ =& [Z^n | H^m] W^m \end{aligned} \tag{10}$$

There are four core parameters for BLS: the number of feature windows W, the number of feature nodes F, the number of enhanced nodes E, and the ridge regression regularization value C for pseudo-inverse. Since the BLS model does not use backpropagation for parameter learning, it obtains the output weight W_{out} by seeking the pseudo-inverse, which means that the initial parameters of the BLS play a vital role in the output weight of the network. Meanwhile, the BLS with a high-quality parameter combination can output the predicted value stably and accurately. Here, we use the PSO algorithm to optimize the BLS and find the most suitable initial parameters for each country and then import the BLS for prediction. The specific process is shown in the algorithm 2 and Figure 4.

IV. Experimental results

In this study, four deep learning models (ANN, CNN, LSTM and GRU) were adopted to compare with the PSO-BLS model. We use $RMSE, MAE, R2$ as the evaluation

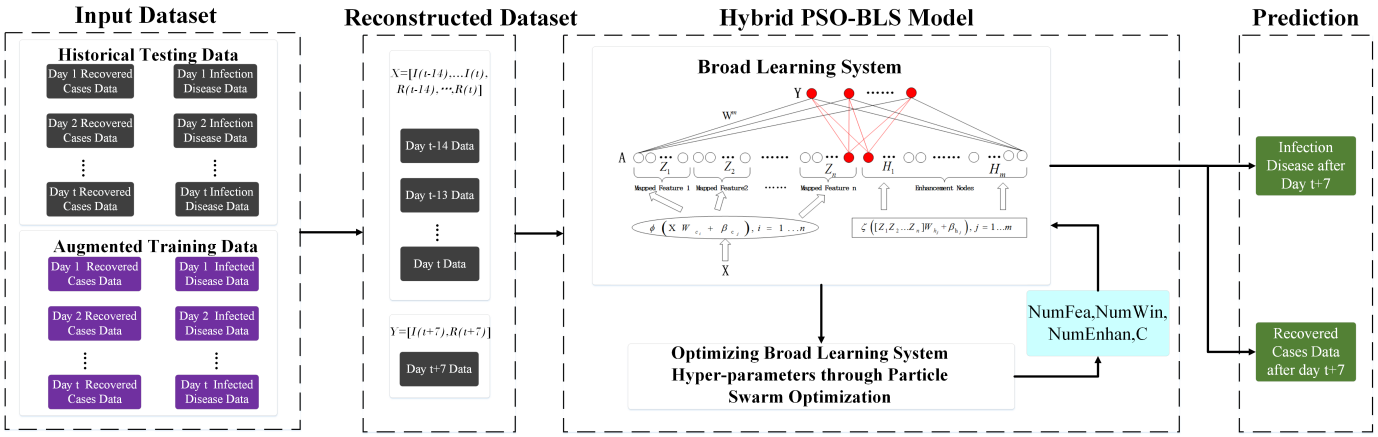

Figure 4. Hybrid PSO-BLS model for COVID-19 forecasting in 184 countries.

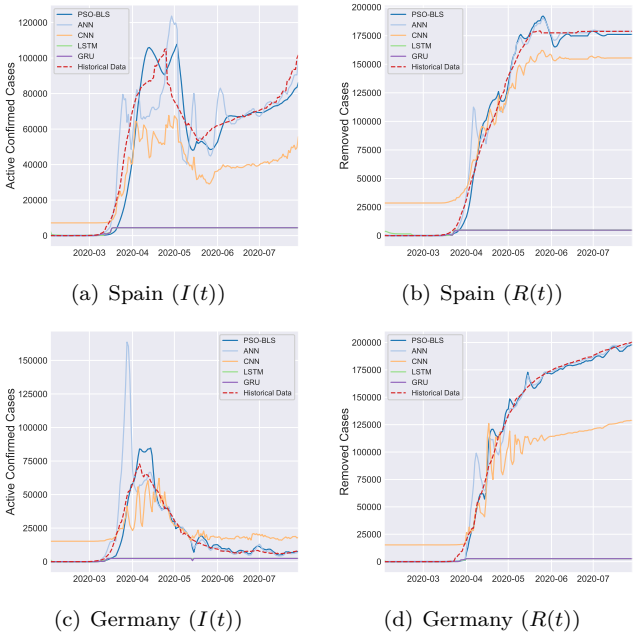

(a) Spain ($I(t)$) (b) Spain ($R(t)$)

(c) Germany ($I(t)$) (d) Germany ($R(t)$)

Figure 5. Prediction results of deep learning model and PSO-BLS model in Croatia, Germany and Argentina.

Table I
EXPERIMENTAL RESULTS OF THE STATE-OF-ART ALGORITHM FOR PREDICTION OF ACTIVE INFECTED CASES IN CROATIA, SPAIN, SOUTH KOREA, AND GERMANY.

Country	Model	*RMSE*	*MAE*	*R2*
Croatia	PSO-BLS	136.978	116.906	0.907
	ANN	436.438	197.511	0.053
	CNN	4192.466	4184.963	-86.385
	LSTM	**130.787**	**91.165**	**0.915**
	GRU	171.992	115.661	0.853
Spain	PSO-BLS	**11150.418**	**7228.758**	**0.890**
	ANN	13866.232	8318.905	0.830
	CNN	25395.119	21884.663	0.429
	LSTM	58818.135	49402.704	-2.065
	GRU	58825.003	49364.759	-2.065
Korea	PSO-BLS	**1177.622**	**599.195**	**0.658**
	ANN	6033.208	1601.960	-7.979
	CNN	14657.027	14571.302	-51.993
	LSTM	1904.8104	1072.478	0.105
	GRU	1914.324	1061.910	0.096
Germany	PSO-BLS	**6064.660**	**3429.111**	**0.908**
	ANN	17442.331	5652.251	0.243
	CNN	12995.350	11087.806	0.580
	LSTM	24941.054	15421.189	-0.548
	GRU	24971.560	15453.019	-0.552

metrics to better evaluate the performance of each model. Table I presents the experimental results of state-of-art algorithms for prediction of active infection cases, while Table II presents the experimental results of prediction of removed cases, and the following experimental conclusions can be drawn:

1) The predictive accuracy of removed cases is higher than the predictive accuracy of active infection cases in each model;
2) The proposed PSO-BLS model has the best predictive performance than the other four deep learning models, with 0.998 for R^2;
3) The PSO-BLS model has higher stability and robustness in various situations. For the prediction of the number of active infection cases, the average R^2 of PSO-BLS can reach 0.892, while for the prediction of the number of removed cases, the average R^2 can reach 0.992. In all cases, the PSO-BLS model has the highest average R^2.

The prediction results generated by ANN, CNN, LSTM, GRU, and PSO-BLS are shown in Figure 5. Here, we adopt two representative countries, including Spain and Germany. Results reveal that the predictive results of ANN and CNN are unstable, while the generalization ability of LSTM and GRU is insufficient. Therefore, the performance of these methods in predicting the number of active infected cases and the number of removed cases is relatively unsatisfactory. However, the PSO-BLS model has higher stability and robustness. The prediction results are consistent with the trend of historical data so that it can predict the number of COVID-19 active infection cases and the number of removed cases more accurately.

V. CONCLUSION

In this study, a particle swarm algorithm-based Broad Learning System (PSO-BLS) was proposed to predict the

Table II
EXPERIMENTAL RESULTS OF THE STATE-OF-ART ALGORITHM FOR PREDICTION OF REMOVED CASES IN CROATIA, SPAIN, SOUTH KOREA, AND GERMANY.

Country	Model	*RMSE*	*MAE*	*R*2
Croatia	PSO-BLS	**108.173**	**80.703**	**0.992**
	ANN	139.331	95.275	0.986
	CNN	25872.577	25856.990	-475.136
	LSTM	828.525	588.574	0.512
	GRU	818.956	523.482	0.523
Spain	PSO-BLS	**6894.854**	4759.910	**0.992**
	ANN	9018.762	**3934.652**	0.987
	CNN	22460.331	21382.969	0.918
	LSTM	125847.041	100035.744	-1.577
	GRU	125855.852	99818.427	-1.578
Korea	PSO-BLS	**489.634**	**0.779**	**0.989**
	ANN	798.840	289.396	0.976
	CNN	7599.815	7031.374	-1.573
	LSTM	7034.5965	5813.314	-1.204
	GRU	7059.165	5821.311	-1.2198
Germany	PSO-BLS	**5891.619**	**3432.747**	**0.995**
	ANN	8951.795	3817.620	0.988
	CNN	45283.7424	37782.707	0.694
	LSTM	129128.684	100798.186	-1.491
	GRU	129157.261	100805.745	-1.493

number of COVID-19 active infected cases and removed cases in 184 countries. Furthermore, we use the S-G Filter algorithm to detect a secondary outbreak in the country and propose a particle swarm algorithm-based infectious disease dynamics model (PSO-SIR) to generate a large number of augmented data. Compared with classical deep learning (DL) algorithms, the PSO-BLS model has a better performance. Moreover, the PSO-BLS algorithm can effectively adapt to predicting complex epidemic disease situations and accurately predict the outbreak trend of COVID-19, even under the outbreak of multiple waves. The proposed PSO-BLS can be extended and suitable for other epidemic prediction problems.

ACKNOWLEDGMENT

This work was supported by National Science Foundation of China Project 61703355 and Science and Technology Program of Guangzhou, China (201904010224 and 201804010292), and Natural Science Foundation of Guangdong Province, China (2020A1515010761).

REFERENCES

[1] R. Wölfel, V. M. Corman, W. Guggemos, M. Seilmaier, S. Zange, M. A. Müller, D. Niemeyer, T. C. Jones, P. Vollmar, and C. Rothe, "Virological assessment of hospitalized patients with COVID-2019," *Nature*, vol. 581, no. 7809, pp. 465–469, 2020.

[2] N. Zhu, D. Zhang, W. Wang, X. Li, B. Yang, J. Song, X. Zhao, B. Huang, W. Shi, R. Lu, *et al.*, "A novel coronavirus from patients with pneumonia in china, 2019," *New England Journal of Medicine*, 2020.

[3] J. F.-W. Chan, S. Yuan, K.-H. Kok, K. K.-W. To, H. Chu, J. Yang, F. Xing, J. Liu, C. C.-Y. Yip, R. W.-S. Poon, *et al.*, "A familial cluster of pneumonia associated with the 2019 novel coronavirus indicating person-to-person transmission: a study of a family cluster," *The Lancet*, vol. 395, no. 10223, pp. 514–523, 2020.

[4] M. U. Kraemer, C.-H. Yang, B. Gutierrez, C.-H. Wu, B. Klein, D. M. Pigott, L. Du Plessis, N. R. Faria, R. Li, W. P. Hanage, *et al.*, "The effect of human mobility and control measures on the COVID-19 epidemic in China," *Science*, vol. 368, no. 6490, pp. 493–497, 2020.

[5] S. Chen, Z. Zhang, J. Yang, J. Wang, X. Zhai, T. Bärnighausen, and C. Wang, "Fangcang shelter hospitals: a novel concept for responding to public health emergencies," *The Lancet*, vol. 395, no. 10232, pp. 1305–1314, 2020.

[6] Worldmeter.com, "Coronavirus cases by country, territory, or conveyance.," 2020.

[7] C. Zhan, C. K. Tse, Z. Lai, X. Chen, and M. Mo, "General model for covid-19 spreading with consideration of intercity migration, insufficient testing, and active intervention: Modeling study of pandemic progression in japan and the united states," *JMIR public health and surveillance*, vol. 6, no. 3, p. e18880, 2020.

[8] A. Pan, L. Liu, C. Wang, H. Guo, X. Hao, Q. Wang, J. Huang, N. He, H. Yu, X. Lin, *et al.*, "Association of public health interventions with the epidemiology of the covid-19 outbreak in wuhan, china," *Jama*, vol. 323, no. 19, pp. 1915–1923, 2020.

[9] C. Zhan, C. Tse, Z. Lai, T. Hao, and J. Su, "Prediction of covid-19 spreading profiles in south korea, italy and iran by data-driven coding," *PLoS ONE*, vol. 15, no. 7, p. e0234763, 2020.

[10] J. Kennedy and R. Eberhart, "Particle swarm optimization," in *Proceedings of ICNN'95-International Conference on Neural Networks*, vol. 4, pp. 1942–1948, IEEE, 1995.

[11] O. Diekmann, H. Heesterbeek, and T. Britton, *Mathematical Tools for Understanding Infectious Disease Dynamics*. Princeton University Press, 2013.

[12] M. Small, P. Shi, and C. K. Tse, "Plausible models for propagation of the SARS virus," *IEICE Transactions on Fundamentals of Electronics, Communications and Computer Sciences*, vol. 87, no. 9, pp. 2379–2386, 2004.

[13] C. P. Chen and Z. Liu, "Broad learning system: An effective and efficient incremental learning system without the need for deep architecture," *IEEE transactions on neural networks and learning systems*, vol. 29, no. 1, pp. 10–24, 2017.

[14] W. H. Organization, "Coronavirus disease (covid-19) outbreak.," 2020.

[15] R. W. Schafer, "What is a savitzky-golay filter?[lecture notes]," *IEEE Signal processing magazine*, vol. 28, no. 4, pp. 111–117, 2011.

[16] C. Zhan, K. T. Chi, and M. Small, "A general stochastic model for studying time evolution of transition networks," *Physica A: Statistical Mechanics and its Applications*, vol. 464, pp. 198–210, 2016.

[17] C. Zhan and L. F. Yeung, "Parameter estimation in systems biology models using spline approximation," *BMC systems biology*, vol. 5, no. 1, p. 14, 2011.

[18] C. Zhan, W. Situ, L. F. Yeung, P. W.-M. Tsang, and G. Yang, "A parameter estimation method for biological systems modelled by ode/dde models using spline approximation and differential evolution algorithm," *IEEE/ACM transactions on computational biology and bioinformatics*, vol. 11, no. 6, pp. 1066–1076, 2014.

[19] Y.-H. Pao, G.-H. Park, and D. J. Sobajic, "Learning and generalization characteristics of the random vector functional-link net," *Neurocomputing*, vol. 6, no. 2, pp. 163–180, 1994.

[20] B. Igelnik and Y.-H. Pao, "Stochastic choice of basis functions in adaptive function approximation and the functional-link net," *IEEE Transactions on Neural Networks*, vol. 6, no. 6, pp. 1320–1329, 1995.